RESEARCH ARTICLE DOI: 10.1002/adsc.202100373

Advanced Synthesis & Catalysis

Visible Light-Mediated Functionalization of Selenocystine-Containing Peptides

Sindija Lapcinska,[a] Pavels Dimitrijevs,[a] Linards Lapcinskis,[b] and Pavel Arsenyan[a,*]

[a] Latvian Institute of Organic Synthesis, Aizkraukles 21, LV-1006, Riga, Latvia
E-mail: pavel@osi.lv

[b] Research Laboratory of Functional Materials Technologies Faculty of Materials Science and Applied Chemistry, Riga Technical University, P. Valdena 3/7, LV-1048, Riga, Latvia

Manuscript received: April 29, 2021; Revised manuscript received: April 29, 2021;
Version of record online: ■■, ■■

Supporting information for this article is available on the WWW under https://doi.org/10.1002/adsc.202100373

Abstract: A straightforward and atom-economic method for the functionalization of short selenocystine-containing peptides is presented. This method is shown to be tolerant to unprotected peptides. The detailed protocol is based on the generation of a selenium radical via visible light-initiated reaction in the presence of transition metal-free photocatalyst. The selenium radical is further oxidized to an electrophile and trapped by *N*-heterocycles. The mechanism is confirmed by NMR, HRMS, UV, EPR and cyclic voltammetry (CV) experiments and photocatalyst emission quenching studies. A visible light-initiated reaction is employed for the synthesis of selenocysteine-containing indole-based macrocycles via intramolecular Se–C bond formation.

Keywords: Macrocycle; *N*-heterocycle; peptide; photocatalysis; selenocysteine

Introduction

Visible light photocatalysis is a rapidly emerging field with attractive advantages such as efficiency, sustainability, atom economy, and selectivity.[1–3] Most organic molecules do not absorb visible light; therefore, the presence of photosensitizers such as transition metal complexes,[4–6] organic dyes[7] or semiconductors[8] facilitates the reaction.

A vast array of methods[9] for synthesis of 3-selenylindoles have been demonstrated employing metal salts (e.g. $FeCl_3$,[10] CuI[11]), bases[12,13] or oxidants.[14–16] More sustainable methods have been developed based on electrochemically-induced process.[17,18]

In the last few years, visible light-mediated C–H functionalization of (hetero)arenes with simple, mainly diaryl diselenides has been reported. Two catalysts outperform others in terms of efficiency of selenylation of indoles and other (hetero)arenes using blue LED light: FIrPic[19] and Rose Bengal[20,21] (RB). Notably, photocatalyst-free selenylation of indole can be performed by prolonged irradiation in ethanol[22] or in methanol under flow conditions.[23] Another green method for selenylation of allenes[24] and (hetero)arenes[25] has been established using LiCl as an additive and a household white LED lamp (λ = 430–730 nm) as the light source. The abovementioned methods were limited solely to the use of diorganyl diselenides, whereas photocatalyst- and additive-free methods for the synthesis of 3-selenyl-, 3-tellanyl-, 3-sulfenyl- and 3-thiocyanoindoles were achieved by employing 26 W CFL bulbs or sunlight, resulting in similar reaction yields.[26] Alternatively, 3-sulfenyl and 3-selenylindoles can be obtained by visible light-induced chalcogenylation of indolines in the presence of graphene oxide.[27]

An indole ring was formed via 5-*endo-dig* cyclization starting from alkynylanilines and diaryl diselenides or disulfides in the presence of H_2O_2 and blue LED light.[28] A simple method for the construction of various heterocycles, e.g., oxazoline, isoxazoline, pyrrolidine, and lactone, was established using diorganyl diselenides and alkene-containing substrates and employing 4-CzIPN and blue LED light to initiate the reaction.[29] Catalyst-free synthesis of arylselanyl- and arylsulfenyl-3,3-difluoro-γ-lactams was demonstrated in the presence of a base (KH_2PO_4).[30] Notably, functionalization of styrenes was demonstrated using diaryl diselenides in the presence of RB by irradiating the mixture with blue LEDs.[31] Visible light-initiated

generation of selenyl radicals with subsequent addition to terminal[32,33] or internal[34] alkynes has also been investigated. Significantly, catalyst-free conditions can be used to realize both visible light-induced metathesis reactions between diselenides and ditellurides[35] and diselenide metathesis between simple diorganyl diselenides[36] or Se–Se bond-containing peptides.[37] Strikingly, there has been no profound study on selenocysteine (Sec)-containing peptide modification under visible light conditions.

Late-stage modification of peptides is not an easy task; however, photocatalysis can provide a route to achieve chemoselective bioconjugation under mild and often biocompatible conditions.[38–41] However, other methods of Sec-containing peptide functionalization have been successfully employed, and common modifications of Sec in selenoproteins have been recently reviewed.[42,43] UV light (254 nm) irradiation of selenocystine-based peptides converts Se–Se bridges to selenolanthionine fragments.[44] Deselenylation of Sec-containing peptides can be effectively achieved by reduction of Sec to alanine with TCEP/DTT[45] or oxidation of Sec to dehydroalanine derivatives with hydrogen peroxide.[46] Notably, an elegant method has been established for Sec-containing peptides and small molecule conjugation based on the electrophilic character of (5-nitropyridylthio)-Sec-containing peptides.[47] Recently, Sec-containing peptide modification through the generation of selenyl electrophiles using weak Lewis acids or oxidants has been demonstrated.[48,49]

Here, we report our findings regarding Se–Se bond-containing peptide modification using visible light-initiated reactions, scope and limitation studies, formation of macrocyclic Sec-containing peptides, and mechanistic studies.

Results and Discussion

Dipeptide dimers Boc-Sec-Gly-OBn **1 a** and 1*H*-indole (**2 a**) were chosen as model substrates to optimize the reaction conditions. Preliminary screening of a photocatalyst panel (more than 25, ESI Figure S1) was performed in acetonitrile using 0.5 equiv. **1 a**, 1 equiv. **2 a**, 2 mol% transition metal catalyst or 5 mol% organic dye and irradiating the reaction mixture with blue LED light (max 461 nm, bright blue, x = 01440, y = 0.0395, > 50 000 lx) for 90 min. The absence of a photocatalyst resulted in no reaction and only a trace amount of desired product **3 a** (Scheme 1). Evaluation of the obtained data led to the conclusion that the popular transition metal catalysts FIrPic and Ru(bpy)$_3$Cl$_2$ were nonselective and provided a mixture of products, including **3 a**. However, a series of fluorescein derivatives, which are well-known organic dyes, were more promising. Fluorescein itself has very low solubility in MeCN; thus, DMF was added. Unfortunately, the formation of the desired product was not observed, although ethyl eosin was capable of inducing the formation of **3 a** (22%). Gratifyingly, RB and erythrosin B induced a full conversion of the starting materials and selective synthesis of 3-selanyl indole **3 a** in just 90 min.

The following catalysts were found to be unsuitable: 5-carboxytetramethylrhodamine (5-TAMRA), nickel tetraphenyl porphyrin, 4-CzIPN, cresol red, chlorophenol red, bromocresol green, methyl orange, congo red, direct red 81, direct yellow 27, methylene blue, basic fuchsine, indigo carmine, alcian blue, 2,4,6-triphenylpyrylium tetrafluoroborate, 9-mesityl-10-methyl acridinium tetrafluoroborate, acridine, and *N*-methyl-acridinium iodide. In most cases, the formation of **3 a** was observed; however, the reaction was nonselective, and the conversion of starting materials was less than 50%. Thus, RB was selected as the most suitable catalyst. The reduction in the catalyst load to 2 mol% resulted in a prolonged reaction time and decrease in yield. Unfortunately, the use of greener protic solvents such as MeOH, EtOH, EtOH/H$_2$O, and *i*PrOH resulted in a nonselective reaction due to the fast oxidation and deselenylation of **1 a**. Changing the light source to a CFL bulb resulted in a significantly slower reaction, whereas a red LED was incapable of initiating the formation of **3 a**. Control tests showed that the reaction did not occur under daylight or dark conditions; thus, the necessity of the LED$_{460}$ light was confirmed. The reaction under an Ar atmosphere did not differ from the reaction performed in an open flask, whereas the reaction in the presence of 4-amino-TEMPO did not result in the formation of **3 a**, confirming the radical mechanism for this process. In summary, the optimized conditions for the synthesis of 3-Sec-indoles were found to be 5 mol% RB, MeCN and blue LED light for 90 min.

To determine how the substituents in the indole ring affect the reaction, we tested the reaction of **1 a** with various indoles. Notably, the presence of an electron-donating group (EDG) at the C5 position of indole improved the reaction yield; halogen atoms did not significantly affect the process, whereas the presence of an electron-withdrawing group (EWG) diminished the reactivity and provided only trace amounts of the products. An EDG at the C2 position provided the product in lower yield, but electron-deficient indoles (EWG at the N1 or C2 position) were completely unreactive. Tripeptide dimer **1 b** showed an even better ability to react with indoles than **1 a**, and the corresponding products **3 k–n** and **3 p** were obtained in excellent yields. Importantly, a hydroxy group at the C5 position of indole was also tolerated under the reaction conditions, although the reaction yield was lower because prolonged irradiation was required for full conversion of the starting materials, whereas the reaction with 5-aminoindole failed, probably due to enamine-imino tautomerism. However, the use of *tert*-

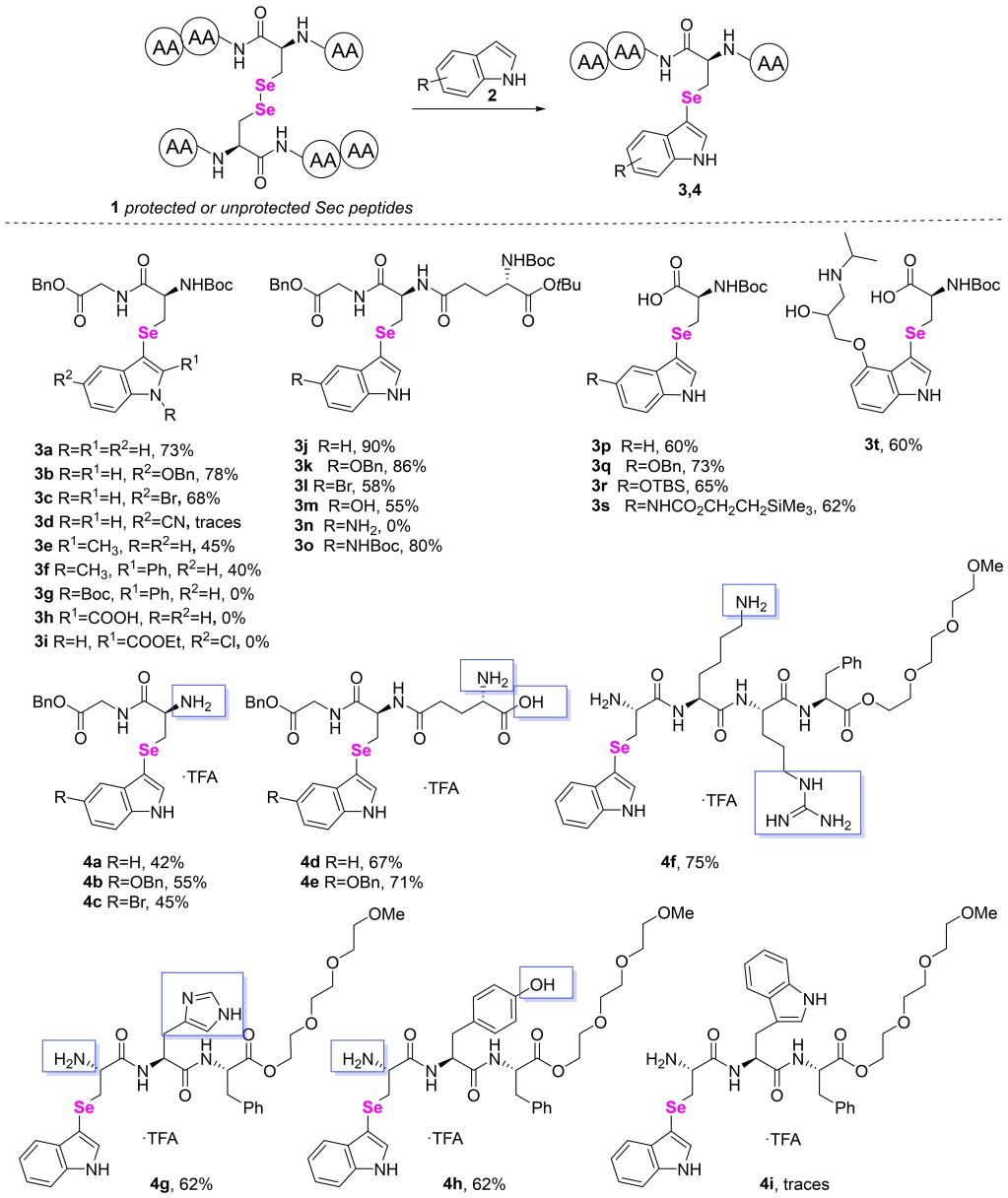

Scheme 1. Sec-indole formation: scope and limitation studies. Reaction conditions: indole **2** (1 equiv.), **1** (0.5 equiv.), RB (0.05 equiv.), blue LED_{460}, MeCN. **1a** (Boc-Sec-Gly-OBn)$_2$, **1b** (Boc-Glu(O*t*Bu)-Sec-Gly-OBn)$_2$, **1c** (Boc-Sec)$_2$, **1d** (H_2N-Sec-Gly-OBn·TFA)$_2$, **1e** (H_2N-Glu(OH)-Sec-Gly-OBn·TFA)$_2$, **1f** (H_2N-Sec-Lys-Arg-Phe-OPEG^{3}OMe·TFA)$_2$, **1g** (H_2N-Sec-His-Phe-OPEG^{3}OMe·TFA)$_2$, **1h** (H_2N-Sec-Tyr-Phe-OPEG^{3}OMe·TFA)$_2$, **1i** (H_2N-Sec-Trp-Phe-OPEG^{3}OMe·TFA)$_2$; **2a** 1*H*-indole, **2b** 5-(benzyloxy)indole, **2c** 5-bromoindole, **2d** 5-cyanoindole, **2e** 2-methylindole, **2f** 1-methyl-2-phenylindole, **2g** 1-Boc-2-phenyl-indole, **2h** 1*H*-indole-2-carboxylic acid, **2i** ethyl 5-chloro-1*H*-indole-2-carboxylate, **2j** 5-hydroxyindole, **2k** 5-aminoindole, **2l** *tert*-butyl (1*H*-indol-5-yl)carbamate, **2m** 5-((*tert*-butyldimethylsilyl)oxy)-1*H*-indole, **2n** 2-(trimethylsilyl)ethyl (1*H*-indol-5-yl) carbamate, **2o** pindolol.

butyl (1*H*-indol-5-yl)carbamate **2l** resulted in the formation of desired product **3o** in high yield. Remarkably, we discovered that Boc-selenocystine **1c** can also be employed in visible light-mediated selenylation, leading to a selenium analog of tryptophan **3p** as well as products **3q**–**s**, which can serve as valuable building blocks. Notably, selenylation of pindolol – a nonselective β-adrenergic antagonist[50] – was successful.

Next, unprotected Sec-containing peptides were applied as starting materials to clearly facilitate the use of the developed protocol. Consequently, utilization of unprotected dipeptide dimer **1d** and tripeptide dimer **1e** led to the formation of desired products **4a**–**e**. Encouraged by these results, we decided to test more

sophisticated Sec-containing peptides with "sensitive" amino acid residues to determine their tolerance under the developed reaction conditions. Thus, pegylated tetra- and tripeptide dimers **1f–i** were prepared and employed in visible light-mediated reactions.

We successfully obtained products **4f–h**, confirming that the Lys, Arg, His and Tyr moieties are well tolerated, whereas the reaction with Trp-containing peptide **1i** was nonselective.

To extend the method's scope, the possibilities for selenylation of indole ring bioisosteres – azaindoles **5** – were evaluated. These substrates proved to be significantly less reactive than 1*H*-indole. The formation of product **6a** (8%), along with side products, was observed when 7-azaindole was used; only trace amounts of product **6b** were formed when 4-azaindole was used, whereas 5-azaindole did not lead to product **6c**. Azaindoles[51] are electron-deficient heterocycles and are thus less reactive than indoles; moreover, these substrates might become deactivated due to excited-state tautomerization.[52]

However, protonation of azaindoles changes their electronic properties and promotes the formation of 3-Sec-azaindoles **6a–c** (Scheme 2). We observed significant differences in the reaction rate for different isomers: 1.5 h was needed for 7-azaindole and 24 h was needed for 5-azaindole to achieve 100% conversion.

These results correlate with the pKa of azaindoles: 7-azaindole has the highest acidity, whereas 5-azaindole has the highest basicity.[53] Notably, protonated imidazo[1,2-*a*]pyridine and imidazo[1,2-*a*]pyrimidine were also successfully employed in visible light-induced selenylation, and the structures of products **6d** (CCDC 2054758) and **6e** (CCDC 2054757) were unambiguously confirmed by X-ray analysis (Figure 1A and 1B).

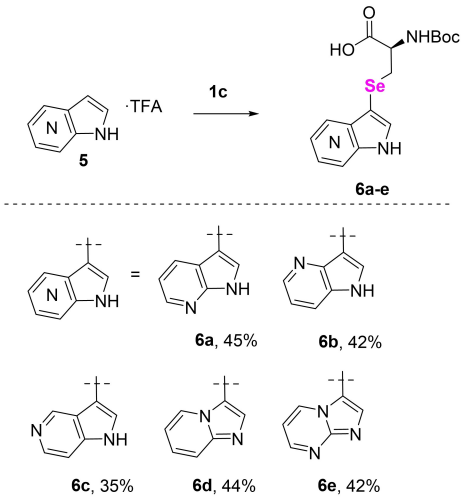

Scheme 2. Synthesis of Sec-azaindoles. Reaction conditions: azaindole **5** (1 equiv.), **1c** (0.5 equiv.), RB (0.05 equiv.), LED_{460}, MeCN.

Next, we were interested in whether the developed protocol can be applied for intramolecular indole selenylation to form Sec-containing peptides with indole-embedded macrocycles. Furthermore, three strategies (Figure 2) were proposed for the formation of macrocycles: (A) visible light-mediated Se–C formation or, in other words, intramolecular indole selenylation; (B) selenylation of an indole attached to the peptide and subsequent intramolecular amide bond formation; and (C) a reaction between Boc-Sec and protected 5-hydroxy- or aminoindole, coupling with a small peptide, deprotection and intramolecular amide bond formation.

First, we intended to prepare Boc-Sec-containing dipeptide and tripeptide dimers (**8**,**9**) attached to the C4 or C5 position of indole through an ester or amide bond. Successive use of **8** and **9** for visible light-mediated intramolecular Se–C bond formation (Approach A) could result in the synthesis of macrocyclic structures **10** (Scheme 3). 1-Methyl-1*H*-indol-4-ol (**2p**) was coupled with Boc-Phe and then deprotected, affording **7a**, which was next coupled with Boc-Sec, yielding **8a**. Gratifyingly, substrate **8a** in the presence of RB under visible light irradiation provided macrocycle **10a** in 60% yield. The intramolecular selenylation proceeded slightly slower than the intermolecular

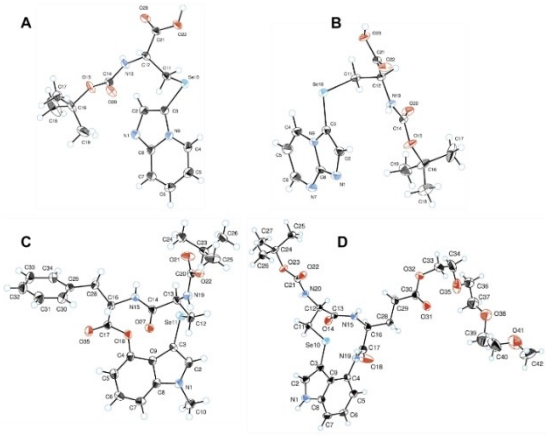

Figure 1. ORTEP molecular structures of **6d** (A), **6e** (B), **10a** (C), **10f** (D).

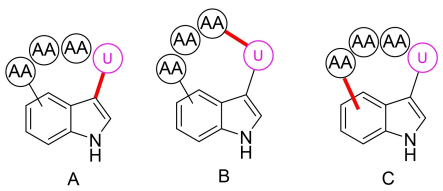

Figure 2. Proposed strategies for Sec-macrocycle formation.

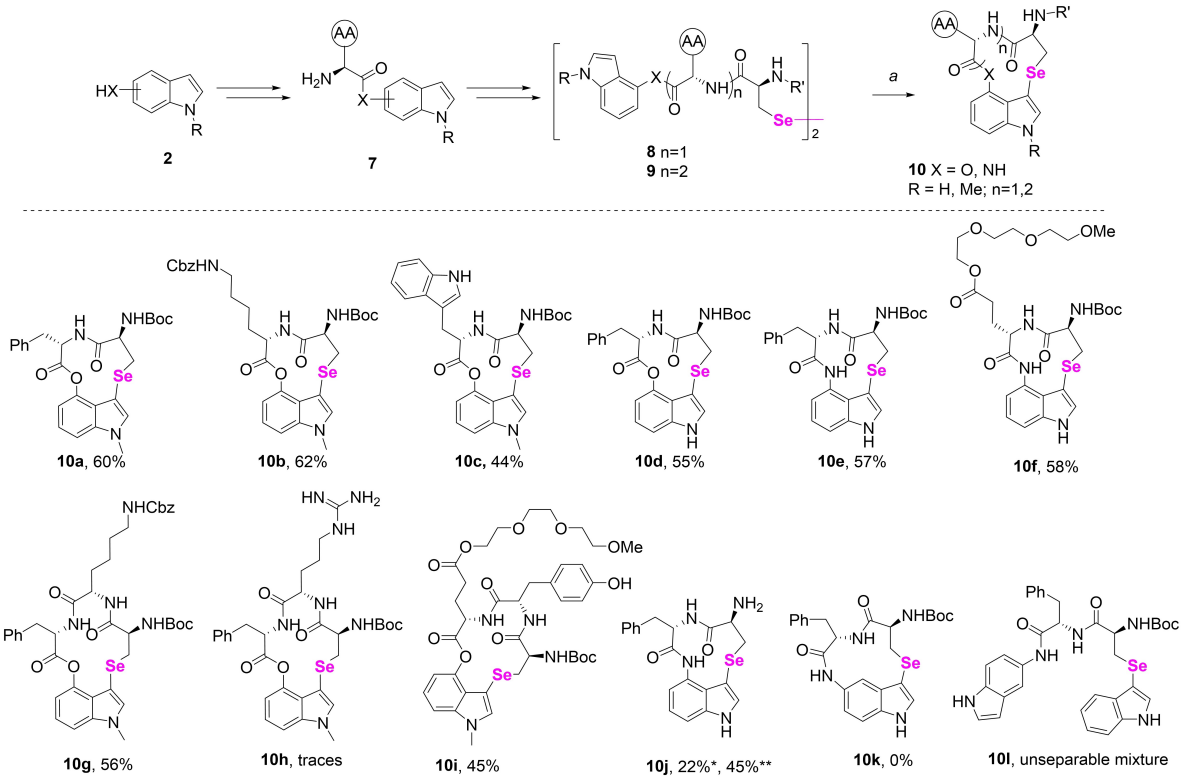

Scheme 3. Synthesis of macrocycles: approach A. Reaction conditions: (a) **8** or **9** (1 equiv.), RB (0.1 equiv.), LED_{460}, MeCN. *Fmoc cleavage, cyclization, **cyclization, Fmoc cleavage.

reaction, but it was selective. Furthermore, the structure of **10a** (CCDC 2054762) was unambiguously confirmed by X-ray analysis (Figure 1C). Macrocycle with *N*(ε)-protected lysine **10b** was successfully synthesized, as was the tryptophan moiety containing macrocycle **10c**, although the yield was slightly lower due to the formation of side products. Next, we tested whether a Sec-containing peptide derivative with 1*H*-indole **8d** can be used to prepare macrocycles. Fortunately, the desired products were obtained starting from 4-hydroxyindole (**2q**) and 4-amino-1*H*-indole (**2r**). Compounds **10a–e** exhibited relatively low solubility; therefore, PEGylated glutamic acid was employed to resolve this issue. The molecular structure of **10f** (CCDC 2054761) was also confirmed by X-ray analysis (Figure 1D). Next, we investigated the preparation of macrocycles that contained tripeptides attached to the indole. Product **10g** containing a Boc-Sec-Lys-Phe moiety was successfully obtained, whereas Arg-containing substrate **9b** was insoluble in MeCN; consequently, the reaction did not occur, but the addition of DMF resulted in a nonselective reaction that yielded only trace amounts of the product **10h**. Fortunately, the introduction of tyrosine (substrate **9c**) was well tolerated under the reaction conditions, resulting in the successful isolation of Tyr-containing macrocycle **10i**. Unfortunately, the Boc protection strategy was unsuitable for the synthesis of unprotected macrocycles due to the instability of indoles under acidic conditions; after protonation, they formed dimers and trimers. However, the preparation of unprotected macrocycle **10j** was accomplished by employing a Fmoc protection strategy. Irradiation of **8g** with LED_{460} light in the presence of RB resulted in the formation of the corresponding macrocycle, and subsequent cleavage of the Fmoc group yielded unprotected macrocycle **10j**. The same product was also obtained by deprotection of **8g** followed by a macrocyclization reaction.

In this case, **10j** was obtained in lower yield; therefore, the advisable sequence for the preparation of unprotected Sec macrocycles is macrocyclization and then deprotection.

Next, the synthesis of Sec macrocycles with a short peptide at the C5 of indole was evaluated. For this purpose, substrate **8h** was irradiated with LED_{460} light. Unfortunately, the formation of product **10k** was not observed. However, we confirmed that intermolecular selenylation can be performed using **8h**. The addition of 1*H*-indole to the reaction mixture of **8h** and RB resulted in the formation of indole derivative **10l**, along with many side products. The results led us to conclusion that strategy A is not suitable for macrocycle formation starting from indoles with peptides

attached to its C5 position, probably due to conformational restrictions.

Approach B to prepare Sec-containing macrocycles relied on visible light-mediated selenylation of indoles **7** that contained the amino acid at the C4 or C5 position of the indole ring and subsequent intramolecular peptide bond formation using standard coupling conditions (Scheme 4). We were keen to investigate whether this synthesis pathway could lead to the formation of macrocycles in which amino acids are attached to the C5 position of indole due to the failed attempt to prepare these macrocycles through approach A.

First, a mixture of Boc-Sec and indole **7h** with PEGylated Glu at the C4 position was irradiated in the presence of RB. The synthesis resulted in isolation of Boc-Sec-containing indole **11a** in good yield. Next, a routine EDC/HOBt method was used for intramolecular amide bond formation. Macrocycle **12a** was isolated in moderate yield along with bis-macrocyclization product **13a** as the minor product. Then, we moved on to selenylation of indoles that contained Phe at the C5 position of indole. We observed that the attachment of Phe to the C5 position of indole through ester bonds and the subsequent reaction with **1c** led to unstable product **11b**. However, indole **7j** was successfully selenylated, and product **11c** was further used for intramolecular amide bond formation. Surprisingly, only bis-macrocyclization product **13b** was formed in the reaction.

We conceded that if a small peptide instead of a single amino acid residue was attached to the C5 position of indole, it would allow the formation of a macrocycle rather than a bis-macrocyclization product. Thus, selenylation of indole **7l** with a Phe-Lys-Phe moiety resulted in formation of **11d**, and subsequent intramolecular amide bond formation provided bis-macrocyclization product **13c** as a single product.

The third approach (Approach C) involved the use of products **3s** and **3t** that were obtained by visible light-mediated selenylation of protected 5-hydroxy- and 5-aminoindoles and proved to be excellent building blocks for macrocycle formation (Scheme 5). Product **3s** was coupled with dipeptide **14a** and treated with TBAF to obtain the corresponding indole-containing peptide **15a**. Subsequent intramolecular amide bond formation resulted in a mixture of compounds, including bis-macrocyclization product **16**. Apparently, this product was also unstable, similar to the other indoles that contained amino acids attached at the C5

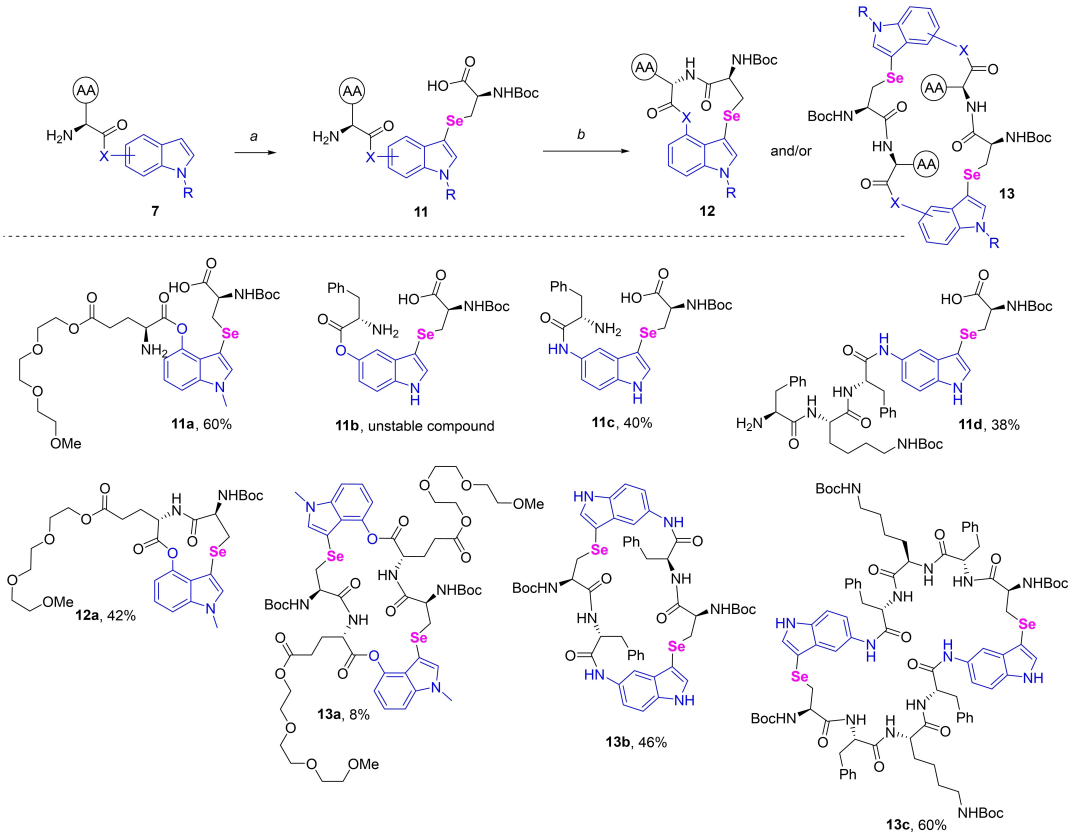

Scheme 4. Synthesis of macrocycles: approach B. (a) indole **7** (1 equiv.), **1c** (0.5 equiv.), RB (0.05 equiv.), LED_{460}, MeCN; (b) **11** (1 equiv.), HOBt (1 equiv.), EDC (1.5 equiv.), DMF.

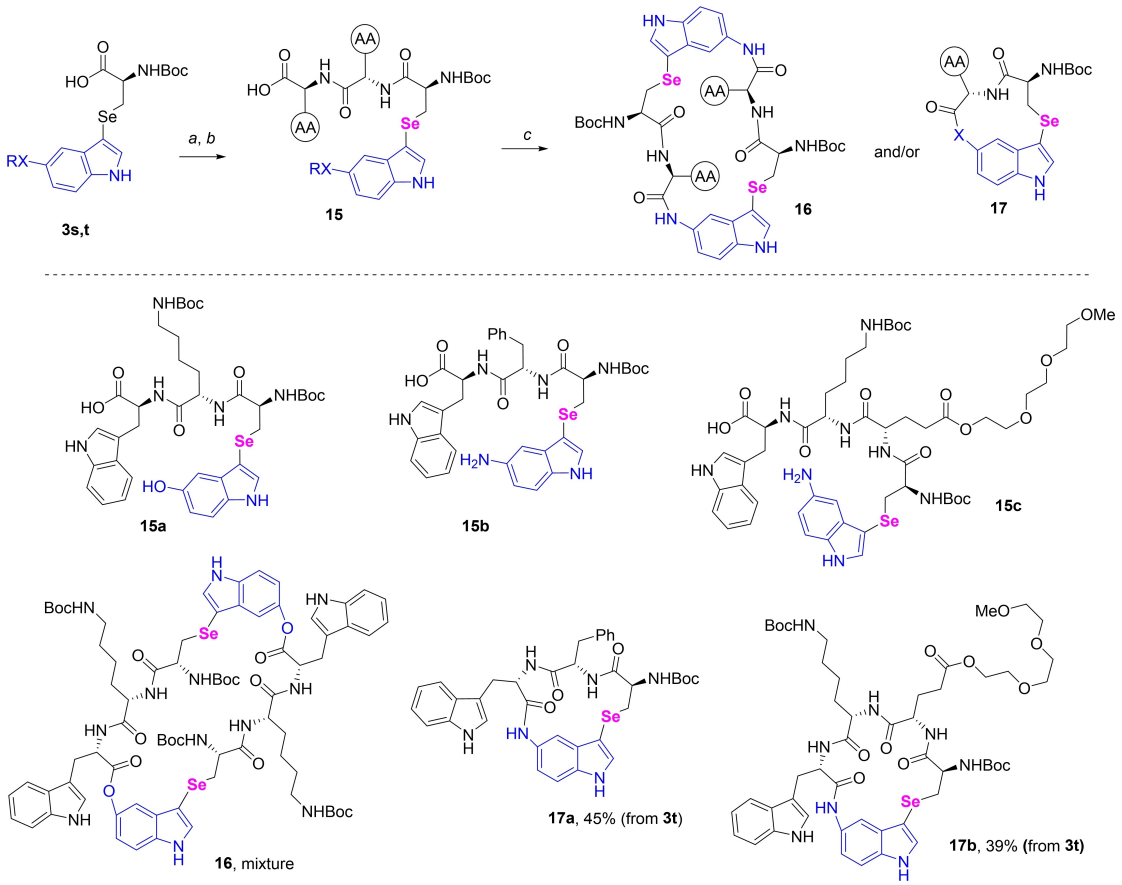

Scheme 5. Synthesis of macrocycles: approach C. Reaction conditions: (a) **3s** or **3t** (1 equiv.), **14** (1 equiv.), HOBt (0.5 equiv.), EDC (1.5 equiv.), DMF; (b) TBAF (3 equiv.), THF; (c) **15** (1 equiv.), HOBt (1 equiv.), EDC (1.5 equiv.), DMF.

position of the indole through an ester bond. Fortunately, stable macrocycles **17a** and **17b** were isolated by employing compounds **15b** and **15c** for intramolecular amide bond formation.

Mechanistic studies. To gain insight into visible light-mediated selenylation, we first examined the possible degradation of Sec-containing peptide **1a** under irradiation. Preliminary tests were performed in acetonitrile, and a solution of **1a** was irradiated with LED_{460} light for 90 min with and without a photocatalyst. No changes were observed in the absence of the photocatalyst, whereas the formation of two products was detected in the presence of RB.

Analysis of the LC/MS data showed that the products were seleninic acid **18** and a dehydroalanine (Dha) derivative **20**, respectively (Scheme 6). On the basis of ^{77}Se NMR spectroscopy data[54] (Figure 3A), alkyl seleninic acid **18** ($RSeO_2H$ 1217.5 ppm, [M+Na]=471.0633) was formed after 1 h of irradiation. Our attempts to isolate oxidized form of **1a** failed due to product lability. Furthermore, storage of an NMR tube for 24 h led to the disappearance of the **18** signal, confirming the formation of seleninic acid (H_2SeO_3 **19**) (1302.7 ppm) and Dha-peptide **20**. The use of Ru-$(bpy)_3Cl_2$ also resulted in the formation of **20**. Other catalysts, namely, FIrPic, ethyl eosin, and 4-CzIPN, induced the formation of **18** and **20** as well but were not able to achieve full consumption of the starting material. 2,4,6 Triphenyl-pyrylium tetrafluoroborate and 9-mesityl-10-methyl-acridinium tetrafluoroborate provided a less selective reaction, whereas DDQ and TAMRA were not efficient. Reactions performed in MeOH, EtOH or DMF did not reach full conversion of **1a** in the given time.

The addition of water did not interfere with the formation of **20**; however, the reaction performed in dry and degassed MeCN under an Ar atmosphere provided a considerably lower conversion of **1a**, thus confirming that the presence of water and oxygen in the solvent is necessary for the reaction to occur. Under irradiation conditions, oxygen is converted to short-living $^1O_2$, returning $RB^{\bullet-}$ to ground state by the energy transfer.[55–58] Singlet oxygen reacts with water generating hydroperoxyl radical that produces hydrogen peroxide,[22] which is trapped by **1a**, resulting in oxidation and deselenylation with the formation of a double bond. The control reaction with TEMPO did not lead to the formation of **20**, thus verifying the

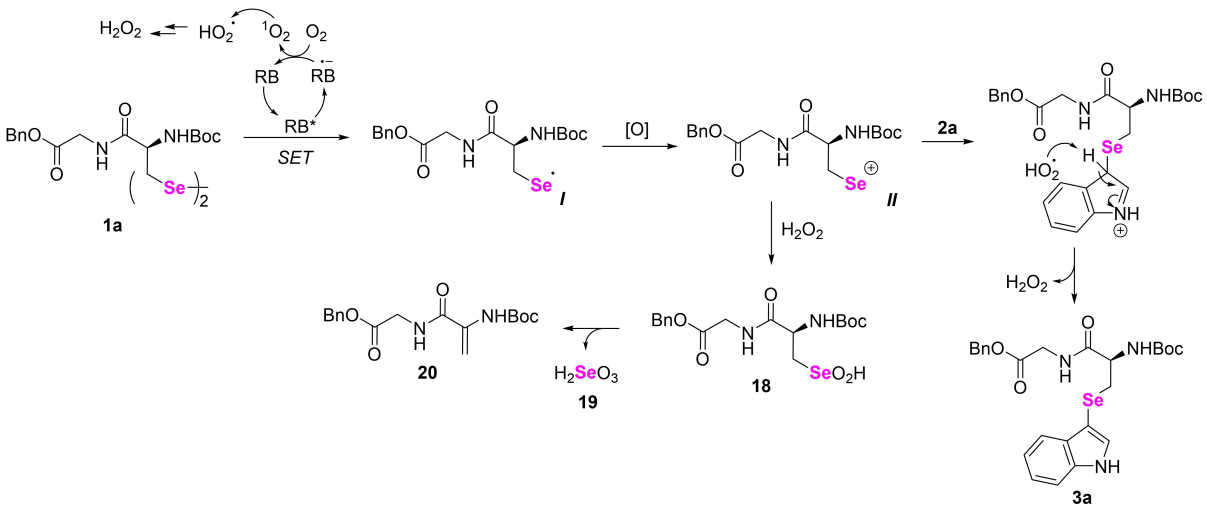

Scheme 6. Proposed mechanism of visible light mediated reaction.

initial radical pathway. On the basis of previously published reports,[19–22,25,26,59] due to differences in reaction conditions, it was problematic to unambiguously specify whether the selenyl radical ***I*** attacks the indole at C3 position, or the indolyl radical is formed first or both selenyl and indolyl radicals are formed simultaneously. To answer this question, the following experiments were performed.

Optical absorption properties. UV spectra were recorded for **1 a**, **2 a**, RB, ethyl eosin, erythrosin B, FIrPic, $Ru(bpy)_3Cl_2 \cdot 6H_2O$, and 4-CzIPN in dry acetonitrile solutions (Figure 3B and 3 C). The photochemical reaction between **2 a** and diselenide **1 a** was not effective in the absence of a catalyst under LED_{460} light because indole has an absorption band from 200 to 305 nm and **1 a** exhibits absorption until 430 nm, albeit with low intensity. Notably, the absorption shoulder at 275–430 nm in the **1 a** UV spectrum is characteristic of Se–Se bonds, which facilitate the formation of selenyl radicals in the presence of a photocatalyst.

Photocatalyst emission quenching. The photoluminescence quenching of RB, $Ru(bpy)_3Cl_2 \cdot 6H_2O$ and FIrPic was performed using **1 a** or **2 a** in degassed acetonitrile. The quenching rate constant of RB in the experiment with **1 a** was determined to be 10.42×10^{-3} l/mol (Figure 3D). In contrast, **2 a** does not quench the fluorescence of RB to any significant extent. Notably, quenching experiments with $Ru(bpy)_3Cl_2 \cdot 6H_2O$ and FIrPic showed the opposite pattern: the **2 a**-quenched fluorescence of both catalysts had a higher Stern-Volmer constant than **1 a** (**2 a**: 5.2×10^{-3} l/mol, **1 a**: 3.6×10^{-3} l/mol of $Ru(bpy)_3Cl_2 \cdot 6H_2O$ (Figure 3E); **2 a**: 0.9×10^{-3} l/mol, **1 a**: 0.5×10^{-3} l/mol of FIrPic) (Figure 3F). Based on the obtained results, it can be concluded that upon excitation of RB, only selenyl radical is formed. Then, selenyl radical ***I*** is oxidized with oxygen to selenyl electrophile ***II***,[19] which is further trapped by **2 a**, resulting in the formation of **3 a** (Scheme 6). Utilization of $Ru(bpy)_3Cl_2 \cdot 6H_2O$ and FIrPic leads to the formation of both selenyl and indolyl radicals, and consequently, an unspecific reaction with the formation of undesired byproducts occurs.

EPR studies. To confirm directly the generation of selenyl radical, EPR studies were conducted. We examined three solutions – RB (50 μM), **1 a** (50 μM), mixture of RB and **1 a** (1:5, 50 μM) in acetonitrile/water (9:1) under LED_{460} light irradiation. Thus, in the absence of light source, no radical formation was detected in the case of RB, **1 a** and the mixture of both (Figure 3G). However, radical formation was confirmed during irradiation of RB in solution ($g = 2.008$, $\Delta H_{pp} = 6G$). The amount of RB* is constant in time. Notably, switching off the light led to disappearance of RB radical. Received data are in agreement with already published research.[58] RB* is not stable and recombines to $RB^* + RB \rightarrow RB^{\bullet+} + RB^{\bullet-}$. Irradiation of **1 a** without photocatalyst did not produce a selenyl radical (Figure 3H). However, the presence of diselenide **1 a** during irradiation, reduced the intensity of RB* signal twice allowing to confirm the establishment of dynamic equilibrium under LED_{460} light: RB* + **1 a** ↔ (RB + **1 a***).

Cyclic voltammetry (CV) studies. To investigate the redox behavior of **1 a** and *N*-heterocycles, as well as the photocatalysts (RB, FIrPic, $Ru(bpy)_3Cl_2 \cdot 6H_2O$), CV studies were performed in dry degassed acetonitrile (details are presented in Table S1 and Figure S2).

The onset oxidation potentials ($E^{ox.vsFc/Fc*}{}_{onset}$) versus Fc were measured by CV from the first redox cycle. The CV of **2 a** shows $E^{ox.vsFc/Fc*}{}_{onset} = 0.43$ V, that of dipeptide **1 a** shows $E^{ox.vsFc/Fc*}{}_{onset} = 0.76$ V, that of RB

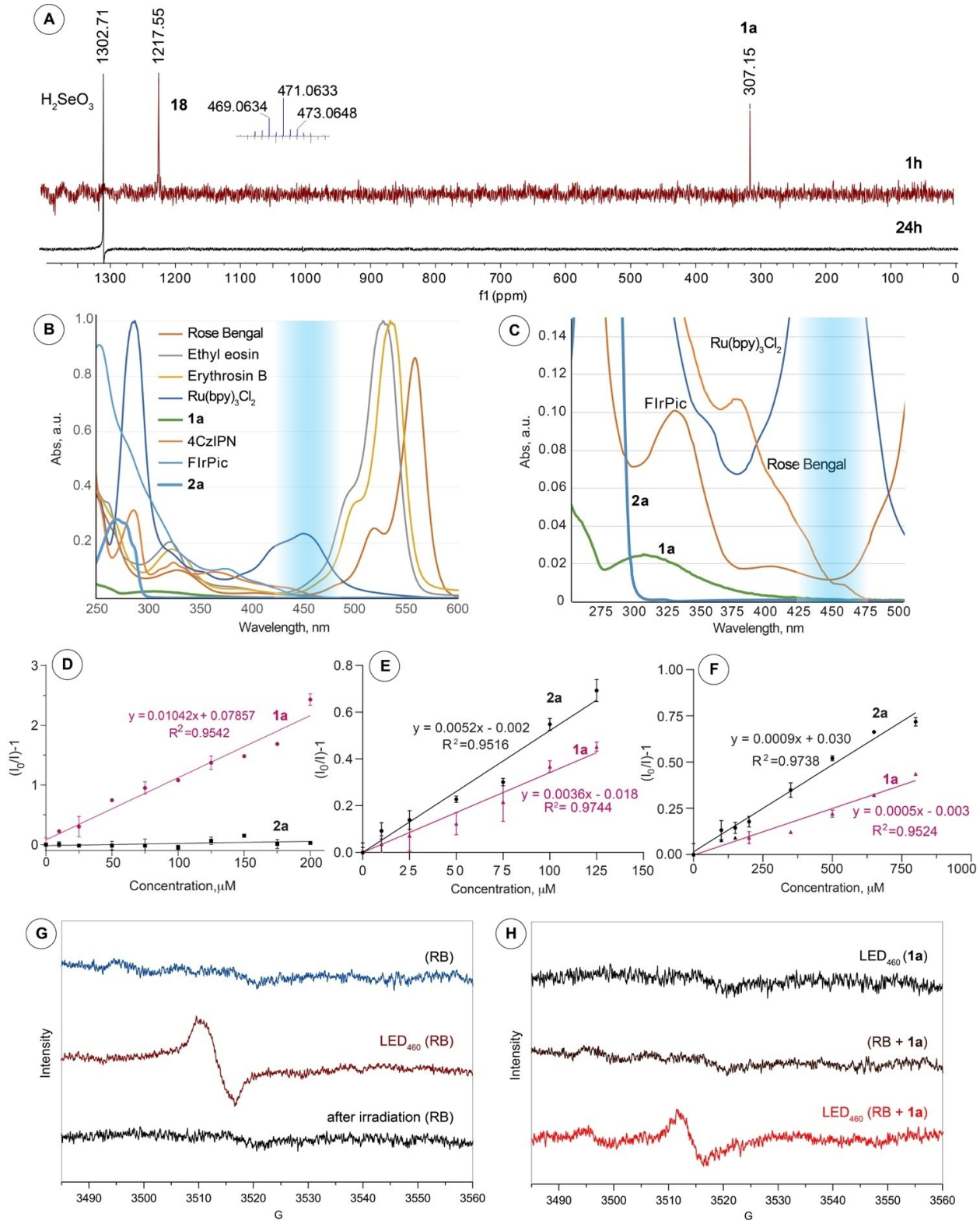

Figure 3. (A) ^{77}Se NMR spectrum of **1a** degradation products after 1 h of irradiation and after storage of the reaction mixture in NMR tube for 24 h; (B) UV spectra of **1a**, **2a** and photocatalysts; (C) Magnified UV spectra of 250–500 nm region (D) Photoluminescence quenching of RB with **1a** and **2a**; (E) Photoluminescence quenching of $Ru(bpy)_3Cl_2 \cdot 6H_2O$ with **1a** and **2a**; (F) Photoluminescence quenching of FIrPic with **1a** and **2a**; (G, H) EPR spectra of RB and RB + **1a** with and without LED_{460} irradiation.

shows $E^{ox.vsFc/Fc*}_{onset} = -0.20$ V and $E^{red.vsFc/Fc*}_{onset} = -1.39$ V, that of FIrPic shows $E^{ox.vsFc/Fc*}_{onset} = 0.73$ V and $E^{red.vsFc/Fc*}_{onset} = 0.94$ V, and that of $Ru(bpy)_3Cl_2 \cdot 6H_2O$ shows $E^{ox.vsFc/Fc*}_{onset} = 0.75$ V and $E^{red.vsFc/Fc*}_{onset} = -1.42$ V. Our experimental data are similar to those in a previously published report,[19] indicating that the photoreaction is mainly initiated by the interaction between the excited photocatalyst and diselenide **1a**. The oxidation potential of **1a** is much higher than the reduction potential of excited RB and $Ru(bpy)_3Cl_2 \cdot 6H_2O$; however, in contrast to that of diphenyl diselenide,[19] the oxidation potential of **1a** matches the reduction potential of FIrPic.[60,61] This result helps explain the low efficiency of FIrPic utilization in light-induced reactions with Sec-containing peptides under the developed reaction conditions. In addition, the redox potentials measured for the studied indoles did not provide clear insight into their reactivity, providing additional evidence that *N*-heterocycles do not involve an electron transfer step from exited RB* and participate solely in the reaction with selenyl electrophile ***II***, yielding Sec-containing peptides.

Conclusion

A straightforward, atom-economic method for the modification of selenocystine peptides was developed. The mechanism of the visible light-mediated reaction was confirmed by NMR, HRMS, UV, EPR and CV experiments and photocatalyst emission quenching studies. The novel method is based on a visible light-initiated reaction for the generation of selenium radical, which is then converted to selenium electrophile that is trapped by electron-rich *N*-heterocyles, thus providing Sec-containing indoles in good yields. Notably, because of initial homolytic cleavage of Se–Se bond the current method allows to utilize both parts of diselenide. Both protected and unprotected Sec-containing peptides can be successfully employed with excellent tolerance for sensitive amino acids (Lys, Arg, His, Glu, Tyr). Furthermore, three approaches were established for the synthesis of Sec-containing indole-based macrocycles. The utilization of visible light provides easy access to simple and sophisticated functionalized Sec-containing peptides, opening the way to a broad application for various types of reactions.

Experimental Section

Representative procedure for visible light-mediated indole selenylation: To a solution of Sec peptide **1a** (100 mg, 0.12 mmol, 0.5 equiv.) and indole **2** (0.24 mmol, 1 equiv.) in MeCN (5 ml) Rose Bengal (12 mg, 0.012 mmol, 0.05 equiv.) was added and the reaction mixture was irradiated by 36 W blue LEDs for 90 minutes. After evaporation the residue was purified by reverse phase flash chromatography (C-18, MeCN/H_2O, 10–85%) to give the product **3**.

CCDC 2054758 (**6a**), CCDC 2054757 (**6e**) CCDC 2054762 (**10a**), CCDC 2054761 (**10f**) contains the supplementary crystallographic data for this paper. These data can be obtained free of charge from The Cambridge Crystallographic Data Centre via www.ccdc.cam.ac.uk/data_request/cif.

Acknowledgements

Financial support from Latvian Institute of Organic Synthesis is gratefully acknowledged (internal grant: IG-2021-01). Authors would like to thank Dr. Sergey Belyakov for X-ray studies and Dr. Larisa Baumane for EPR experiments.

References

[1] X.-Y. Yu, J.-R. Chen, W.-J. Xiao, *Chem. Rev.* **2021**, *121*, 506–561.
[2] J. Xie, H. Jin, A. S. K. Hashmi, *Chem. Soc. Rev.* **2017**, *46*, 5193–5203.
[3] L. Marzo, S. K. Pagire, O. Reiser, B. König, *Angew. Chem. Int. Ed.* **2018**, *57*, 10034–10072; *Angew. Chem.* **2018**, *130*, 10188–10228.
[4] C. K. Prier, D. A. Rankic, D. W. C. MacMillan, *Chem. Rev.* **2013**, *113*, 5322–5363.
[5] T. P. Yoon, M. A. Ischay, J. Du, *Nat. Chem.* **2010**, *2*, 527–532.
[6] F. Strieth-Kalthoff, F. Glorius, *Chem.* **2020**, *6*, 1888–1903.
[7] N. A. Romero, D. A. Nicewicz, *Chem. Rev.* **2016**, *116*, 10075–10166.
[8] H. Kisch, *Angew. Chem. Int. Ed.* **2013**, *52*, 812–847; *Angew. Chem.* **2013**, *125*, 842–879.
[9] A. Ivanova, P. Arsenyan, *Coord. Chem. Rev.* **2018**, *370*, 55–68.
[10] E. Q. Luz, D. Seckler, J. S. Araújo, L. Angst, D. B. Lima, E. A. M. Rios, R. R. Ribeiro, D. S. Rampon, *Tetrahedron* **2019**, *75*, 1258–1266.
[11] B. M. Vieira, S. Thurow, M. Costa, A. M. Casaril, M. Domingues, R. F. Schumacher, G. Perin, D. Alves, L. Savegnago, Eder J. Lenardão, *Asian J. Org. Chem.* **2017**, *6*, 1635–1646.
[12] Y. Yu, Y. Zhou, Z. Song, G. Liang, *Org. Biomol. Chem.* **2018**, *16*, 4958–4962.
[13] Z. Gao, X. Zhu, R. Zhang, *RSC Adv.* **2014**, *4*, 19891–19895.
[14] J. Rafique, S. Saba, M. S. Franco, L. Bettanin, A. R. Schneider, L. T. Silva, A. L. Braga, *Chem. A Eur. J.* **2018**, *24*, 4173–4180.
[15] C. Ding, Y. Yu, Q. Yu, Z. Xie, Y. Zhou, J. Zhou, G. Liang, Z. Song, *ChemCatChem* **2018**, *10*, 5397–5401.
[16] J. B. Azeredo, M. Godoi, G. M. Martins, C. C. Silveira, A. L. Braga, *J. Org. Chem.* **2014**, *79*, 4125–4130.
[17] X. Zhang, C. Wang, H. Jiang, L. Sun, *Chem. Commun.* **2018**, *54*, 8781–8784.

[18] A. G. Meirinho, V. F. Pereira, G. M. Martins, S. Saba, J. Rafique, A. L. Braga, S. R. Mendes, *Eur. J. Org. Chem.* **2019**, 6465–6469.
[19] Q.-B. Zhang, Y.-L. Ban, P.-F. Yuan, S.-J. Peng, J.-G. Fang, L.-Z. Wu, Q. Liu, *Green Chem.* **2017**, *19*, 5559–5563.
[20] S. Saba, J. Rafique, M. S. Franco, A. R. Schneider, L. Espíndola, D. O. Silva, A. L. Braga, *Org. Biomol. Chem.* **2018**, *16*, 880–885.
[21] A. Srivastava, P. K. Singh, A. Ali, P. P. Singh, V. Srivastava, *RSC Adv.* **2020**, *10*, 39495–39508.
[22] I. D. Lemir, W. D. Castro-Godoy, A. Heredia, L. C. Schmidt, J. E. Argüello, *RSC Adv.* **2019**, *9*, 22685–22694.
[23] A. A. Heredia, S. M. Soria-Castro, W. D. Castro-Godoy, I. D. Lemir, M. López-Vidal, F. R. Bisogno, J. E. Argüello, G. Oksdath-Mansilla, *Org. Process Res. Dev.* **2020**, *24*, 540–545.
[24] G. Kumaraswamy, S. Vijaykumar, K. Ankammaa, V. Narayanaraoa, *Org. Biomol. Chem.* **2016**, *14*, 11415–11425.
[25] G. Kumaraswamy, V. Ramesh, M. Gangadhar, S. Vijaykumar, *Asian J. Org. Chem.* **2018**, *7*, 1689–1697.
[26] V. Rathore, S. Kumar, *Green Chem.* **2019**, *21*, 2670–2676.
[27] C. Liu, X. Peng, D. Hu, F. Shi, P. Huang, J. Luo, Q. Liu, L. Liu, *New J. Chem.* **2020**, *44*, 17245–17251.
[28] Q. Shi, Y. Zhang, L. Wang, *Org. Chem. Front.* **2017**, *4*, 1322–1330.
[29] Q.-B. Zhang, P.-F. Yuan, L.-L. Kai, K. Liu, Y.-L. Ban, X.-Y. Wang, L.-Z. Wu, Q. Liu, *Org. Lett.* **2019**, *21*, 885–889.
[30] Z.-P. Ye, P.-J. Xia, F. Liu, Y.-Z. Hu, D. Song, J.-A. Xiao, P. Huang, H.-Y. Xiang, X.-Q. Chen, H. Yang, *J. Org. Chem.* **2020**, *85*, 5670–5682.
[31] J. Chen, R. Chen, L. Mei, S. Yan, Y. Wu, Q. Li, B. Yuan, *Asian J. Org. Chem.* **2020**, *9*, 181–184.
[32] A. C. H. Weber, F. L. Coelho, R. F. Affeldt, P. H. Schneider, *Eur. J. Org. Chem.* **2018**, 6738–6742.
[33] H. Chen, R. Ding, H. Tang, Y. Pan, Y. Xu, Y. Chen, *Chem. Asian J.* **2019**, *14*, 3264–3268.
[34] X.-L. Ma, Q. Wang, X.-Y. Feng, Z.-Y. Mo, Y.-M. Pan, Y.-Y. Chen, M. Xin, Y.-L. Xu, *Green Chem.* **2019**, *21*, 3547–3551.
[35] C. Liu, J. Xia, S. Ji, Z. Fan, H. Xu, *Chem. Commun.* **2019**, *55*, 2813–2816.
[36] S. Ji, W. Cao, Y. Yu, H. Xu, *Angew. Chem. Int. Ed.* **2014**, *53*, 6781–6785; *Angew. Chem.* **2014**, *126*, 6899–6903.
[37] M. Waliczek, Ö. Pehlivan, P. Stefanowicz, *ChemistryOpen* **2019**, *8*, 1199–1203.
[38] C. Bottecchia, T. Noël, *Chem. Eur. J.* **2019**, *25*, 26–42.
[39] J.-Q. Liu, A. Shatskiy, B. S. Matsuura, M. D. Kärkäs, *Synthesis* **2019**, *51*, 2759–2791.
[40] X. Chen, F. Ye, X. Luo, X. Liu, J. Zhao, S. Wang, Q. Zhou, G. Chen, P. Wang, *J. Am. Chem. Soc.* **2019**, *141*, 18230–18237.
[41] H. Choi, M. Kim, J. Jang, S. Hong, *Angew. Chem. Int. Ed.* **2020**, *59*, 22514–22522; *Angew. Chem.* **2020**, *132*, 22703–22711.
[42] R. Mousa, R. N. Dardashti, N. Metanis, *Angew. Chem. Int. Ed.* **2017**, *56*, 15818–15827; *Angew. Chem.* **2017**, *129*, 16027–16037.
[43] E. S. J. Arnér, *Essays Biochem.* **2019**, *64*, 45–53.
[44] M. Waliczek, Ö. Pehlivan, P. Stefanowic, *New J. Chem.* **2020**, *44*, 11433–11436.
[45] X. Wang, A. S. Ashhurst, L. J. Dowman, E. E. Watson, H. Y. Li, A. J. Fairbanks, M. Larance, A. Kwan, R. J. Payn, *Org. Lett.* **2020**, *22*, 6863–6867.
[46] K. M. Reddy, G. Mugesh, *Chem. Eur. J.* **2019**, *25*, 8875–8883.
[47] D. T. Cohen, C. Zhang, C. M. Fadzen, A. J. Mijalis, L. Hie, K. D. Johnson, Z. Shriver, O. Plante, S. J. Miller, S. L. Buchwald, B. L. Pentelute, *Nat. Chem.* **2019**, *11*, 78–85.
[48] P. Arsenyan, S. Lapcinska, A. Ivanova, J. Vasiljeva, *Eur. J. Org. Chem.* **2019**, 4951–4961.
[49] S. Lapcinska, P. Arsenyan, *Eur. J. Org. Chem.* **2020**, 784–795.
[50] P. C. Stafylas, P. A. Sarafidis, *Vasc. Health Risk. Manag.* **2008**, *4*, 23–30.
[51] P. Kannaboina, K. Mondal, J. K. Laha, P. Das, *Chem. Commun.* **2020**, *56*, 11749–11762.
[52] M. T. Cash, P. R. Schreinera, R. S. Phillips, *Org. Biomol. Chem.* **2005**, *3*, 3701–3706.
[53] K. Belasri, F. Fülöp, I. Szatmári, *Molecules* **2019**, *24*, 3578–3587.
[54] M. S. Silva, D. Alves, D. Hartwig, R. G. Jacob, G. Perin, E. J. Lenardão, *Asian J. Org. Chem.* **2021**, *10*, 91–128.
[55] W. Guo, W. Tan, M. Zhao, K. Tao, L. Zheng, Y. Wu, D. Chen, X. Fan, *RSC Adv.* **2017**, *7*, 37739–37742.
[56] G. Brahmachari, I. Karmakar, *J. Org. Chem.* **2020**, *85*, 8851–8864.
[57] T. Sabri, P. D. Pawelek, J. A. Capobianco, *ACS Appl. Mater. Interfaces* **2018**, *10*, 26947–26953.
[58] J. Al–Nu'airat, B. Z. Dlugogorski, X. Gao, N. Zeinali, J. Skut, P. R. Westmoreland, I. Oluwoyeaand, M. Altarawneh, *Phys. Chem. Chem. Phys.* **2019**, *21*, 171–183.
[59] W. Zhang, S. Li, X. Tang, J. Tang, C. Pan, G. Yu, *Appl. Catal. B* **2020**, *272*, 118982.
[60] Y. Zhou, W. Li, Y. Liu, L. Zeng, W. Su, M. Zhou, *Dalton Trans.* **2012**, *41*, 9373–9381.
[61] H. Zhou, P. Lu, X. Gu, P. Li, *Org. Lett.* **2013**, *15*, 5646–5649.

RESEARCH ARTICLE

Visible Light-Mediated Functionalization of Selenocystine-Containing Peptides

Adv. Synth. Catal. **2021**, *363*, 1 – 12

S. Lapcinska, P. Dimitrijevs, L. Lapcinskis, P. Arsenyan*